Central European Science Journals
w w w . c e s j . c o m

Central European Journal of Physics
Central European Science Journals
CEJP 2 (2003) 210–234

The effective absorption cross-section of thermal neutrons in a medium containing strongly or weakly absorbing centres

Krzysztof Drozdowicz, Barbara Gabańska, Andrzej Igielski, Ewa Krynicka, Urszula Woźnicka*

The Henryk Niewodniczański Institute of Nuclear Physics, ul. Radzikowskiego 152, 31-342 Kraków, Poland

Received 24 January 2003; revised 11 February 2003

Abstract: The structure of a heterogeneous system influences diffusion of thermal neutrons. The thermal-neutron absorption in grained media is considered in the paper. A simple theory is presented for a two-component medium treated as grains embedded in the matrix or as a system built of two types of grains (of strongly differing absorption cross-sections). A grain parameter is defined as the ratio of the effective macroscopic absorption cross-section of the heterogeneous medium to the absorption cross-section of the corresponding homogeneous medium (consisting of the same components in the same proportions). The grain parameter depends on the ratio of the absorption cross-sections and contributions of the components and on the size of grains. The theoretical approach has been verified in experiments on prepared dedicated models which have kept required geometrical and physical conditions (silver grains distributed regularly in Plexiglas). The effective absorption cross-sections have been measured and compared with the results of calculations. A very good agreement has been observed. In certain cases the differences between the absorption in the heterogeneous and homogeneous media are very significant. A validity of an extension of the theoretical model on natural, two-component, heterogeneous mixtures has been tested experimentally. Aqueous solutions of boric acid have been used as the strongly absorbing component. Fine- and coarse-grained pure silicon has been used as the second component with well-defined thermal-neutron parameters. Small and large grains of diabase have been used as the second natural component. The theoretical predictions have been confirmed in these experiments.

Keywords: thermal neutrons, absorbing centres, effective absorption, grain parameter, heterogeneity
PACS (2000): 28.20.F, 28.20.G

* E-mail: Urszula.Woznicka@ifj.edu.pl

Contents

1 Introduction

The macroscopic thermal-neutron absorption cross-section Σ_a of a medium is one of several important parameters when the transport of thermal neutrons in any system is considered. The Σ_a value for a homogeneous mixture of n components can be obtained [1] from the simple relation:

$$\Sigma_a = \rho \Sigma_{i=1}^{n} q_i \Sigma_{a_i}^{M} \tag{1}$$

where ρ is the mass density of the mixture, q_i is the mass contribution of the i-th component, ($\Sigma q_i = 1$), and $\Sigma_{a_i}^{M}$ is the mass absorption cross-section of the i-th component (dependent on its elemental composition and the microscopic absorption cross-sections σ_j of the contributing elements, e.g. [2]). Sometimes, it is convenient to express the contributions by the volume contents of components:

$$\phi_i = \frac{V_i}{V} \tag{2}$$

where V_i is the volume occupied by the i-th component in the volume V of the sample. Then Eq. (1), still for the homogeneous mixture, yields:

$$\Sigma_a = \Sigma_{i=1}^{n} \phi_i \Sigma_{a_i} \tag{3}$$

where Σ_{ai} is the macroscopic absorption cross-section of the i-th component, defined at the partial solid material density $\rho_i = m_i / V_i$ (where m_i is the mass of the i-th component in the sample).

In the case of a medium that is a heterogeneous mixture, the effective thermal-neutron absorption can significantly differ from that in a homogeneous one that consists of the same components in the same proportions. A problem of the heterogeneity resulting from the presence of grains in the sample can appear when the absorption cross-section of a rock material is measured. The samples for a neutron experiment are usually prepared by crushing the rocks, and the possible natural heterogeneity can be increased additionally during this procedure. Finally, just an effective cross-section of the heterogeneous sample material is measured. Most often, neither the actual heterogeneity nor the detailed elemental composition is known, and it is impossible to do an exact neutron transport calculation for the medium investigated. On the other hand, it is necessary to introduce a correction to the result of the measurement.

We present here a comprehensive study of the physical problem and its experimental implications. A simple theory of the effective absorption of thermal neutrons in a grained medium is outlined and applied to an interpretation of the pulsed measurement of the absorption cross-section on heterogeneous models (consisting of grains in a matrix, where the geometric structure and the thermalneutron diffusion parameters are well-known). Validity of the theory is further tested and confirmed on more realistic samples of fine and coarse-grained materials: artificial or natural rock grains mixed with a fluid absorbers.

2 Definition of the grain parameter

The material heterogeneity for the thermal-neutron transport in a considered volume is understood here as many small regions that differ significantly in their macroscopic characteristics of neutron diffusion. Being limited to a two-component medium, we distinguish two cases. Case **A**: grains of material 2 dispersed in homogeneous material 1, and Case **B**: a complex medium built of two types of grains (Fig. 1). The volume contribution of substance 2 in the medium is ϕ. Then the macroscopic absorption cross-section Σ_a^{hom} of the corresponding homogeneous, two-component medium of the absorption cross-sections Σ_{a_1} and Σ_{a_2}, respectively, can be obtained from the relation:

$$\Sigma_a^{hom} = (1-\phi)\Sigma_{a_1} + \phi\Sigma_{a_2}. \tag{4}$$

The thermal-neutron absorption in grains of sizes comparable to the neutron mean free path can be no longer described by the macroscopic absorption cross-section relevant for an infinite medium. A modified, effective absorption cross-section of the grains, say $\tilde{\Sigma}_a$, is introduced. In Case **A**, we assume that only the Σ_{a_2} is modified by the grain effect: $\Sigma_{a_2} \to \tilde{\Sigma}_{a_1}$, and the Σ_{a_1} remains unchanged. In Case **B**, both absorption cross-sections are modified: $\Sigma_{a_1} \to \tilde{\Sigma}_{a_1}$ and $\Sigma_{a_2} \to \tilde{\Sigma}_{a_1}$. The effective cross-section Σ_a^{eff} of the entire heterogeneous medium (the grained mixture) is still calculated from formula (4), but with the substitutions mentioned above.

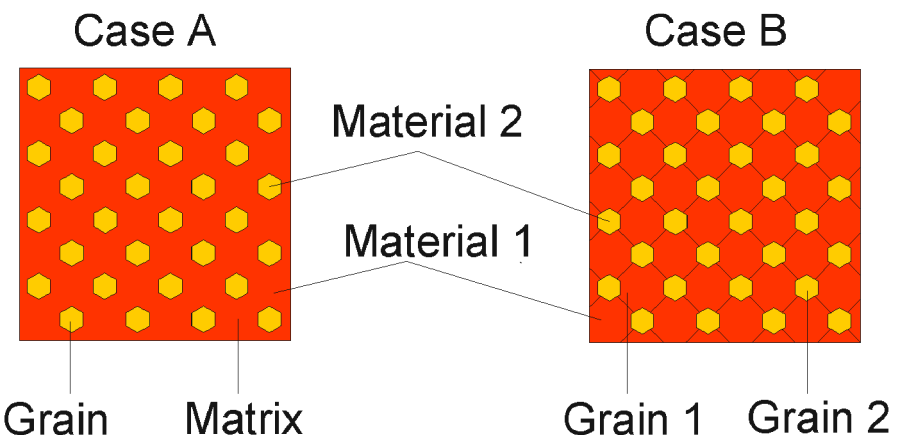

Fig. 1 Two types of the material heterogeneity. Case **A**: grains of material 2 dispersed in homogeneous material 1. Case **B**: material built of two types of grains.

The medium is recognised as *heterogeneous* for the thermal-neutron transport when its effective absorption cross-section Σ_a^{eff} differs from the cross-section Σ_a^{hom} calculated from formula (3), valid for the homogeneous medium. The ratio

$$G = \frac{\Sigma_a^{eff}}{\Sigma_a^{hom}} \tag{5}$$

called the grain effect parameter, defines the heterogeneity effect on the thermal-neutron absorption. The parameter $G = 1$ corresponds to the homogeneous medium. The cross-sections Σ_a^{eff} and Σ_a^{hom} can be theoretically calculated and experimentally measured.

3 Effective absorption cross-section $\tilde{\Sigma}_a$ of grains

We start from a consideration of the thermal-neutron diffusion in a medium within the one-speed approximation. The probability that the neutron is absorbed when it travels a path length x_0 in an absorber is

$$p(x_0) = \int_0^{x_0} e^{-x\,\Sigma_t}\,\Sigma_a\,dx = \frac{\Sigma_a}{\Sigma_t}(1 - e^{-x_0\,\Sigma_t}) \tag{6}$$

(cf. [1] Sec.1.3), where Σ_t is the total cross-section:

$$\Sigma_t = \Sigma_a + \Sigma_s, \tag{7}$$

and Σ_s is the scattering cross-section. In the case of a significant anisotropy of neutron scattering, the transport cross-section can be introduced:

$$\Sigma_{tr} = (1 - \mu) \quad \Sigma_s, \tag{8}$$

where μ is the average cosine of the scattering angle. The total cross-section Σ_t is then substituted by the thermal-neutron diffusion cross-section:

$$\Sigma_d = \Sigma_a + \Sigma_{tr} = \Sigma_t - \mu\Sigma_s. \tag{9}$$

Instead of Eq. (6) we now have

$$p(x_0) = \int_0^{x_0} e^{-x\Sigma_d}\Sigma_a dx = \frac{\Sigma_a}{\Sigma_d}(1 - e^{-x_0\Sigma_d}) \tag{10}$$

Assuming the effective absorption cross-section $\tilde{\Sigma}_a$ in the grain as the absorption probability per unit path length, we obtain from Eq. (10) the following definition:

$$\tilde{\Sigma}_a = \frac{p(\overline{d})}{\overline{d}} = \frac{\Sigma_a}{\overline{d}\Sigma_d}(1 - e^{-\overline{d}\Sigma_d}) \tag{11}$$

where the size of the grain is given by the average chord length $\overline{d}$:

$$\overline{d} = \frac{4V_g}{S_g} \tag{12}$$

and V_g and S_g are the volume and the surface of the grain, respectively [3].

Thus, the effective absorption cross-section of the grain $\tilde{\Sigma}_{a_1}$, besides depending on the absorption properties of the grain substance, also depends on its scattering properties and the size of the grain. Eq. (11) leads to the following two limiting cases. When the size of grains $\overline{d}$ tends to zero (that is, the material becomes homogeneous), $\overline{d}\Sigma_d \to 0$, the absorption cross-section $\tilde{\Sigma}_a \to \Sigma_a$. In another limit, $\overline{d}\ \ \Sigma_d \to \infty$, which corresponds to a thick absorber, the absorption cross-section is

$$\tilde{\Sigma}_a = \frac{\Sigma_a}{\overline{d}\Sigma_d}.$$

Expressions similar to this formula appear when considering the self-shielding effect, when the inner parts of the absorber are partly protected from the incoming neutrons by outer absorbing layers, and neutron scattering is also taken into account (cf. [1] Sec.11.2, [4], [5]).

4 Effective absorption cross-section Σ_a^{eff} of the heterogeneous system

The effective absorption cross-section Σ_a^{eff} of the heterogeneous system in Case **A** is given by the formula:

$$\Sigma_a^{eff} = (1-\phi)\Sigma_{a_1} + \phi\frac{\Sigma_{a_2}}{\overline{d}_2\Sigma_{d_2}}(1-e^{-\overline{d}_2\Sigma_{d_2}}) \tag{13}$$

when the definition of the effective cross-section of the grains, $\tilde{\Sigma}_{a_2}$, is introduced into formula (4).

The substitution of Eqs. (4) and (13) into Eq. (5) yields:

$$G(Y,S,\phi) = \frac{\phi(S\frac{1-e^{-Y}}{Y}-1)+1}{\phi(S-1)+1} \tag{14}$$

where S is the ratio of the absorption cross-sections of the components:

$$S = \frac{\Sigma_{a_2}}{\Sigma_{a_1}} \tag{15}$$

and

$$Y = \overline{d}_2\Sigma_{d_2} \tag{16}$$

is the average size of the grain expressed in the neutron diffusion mean free paths and defines a dimensionless size of the grain.

The parameter G can be studied as a function either of the dimensionless size Y of grains, or of the ratio S of the cross-sections of the contributing materials, or of the material volume content ϕ, depending on which of the variables are fixed as parameters. Examples of the functions defined in Eq. (14) are plotted in Fig. 2. The plot in Fig. 2a shows that the parameter $G(Y)$ can attain a very low value, down to about 0.1 in certain cases, which means that the effective cross-section can be about as low as 10 % of the value for the corresponding homogeneous mixture (for which $Y = 0$ and $G = 1$). Functions $G(S)$ and $G(\phi)$ in Figs. 2b and 2c are plotted for the same grain size $Y = 1$. They show a saturation effect: that means a very weak dependence of G on S or ϕ when they attain sufficiently high values. In the examples presented at a fixed grain size, this weak dependence is observed for $S \geq 100$ (the level depending on ϕ) and for $\phi \geq 0.2$ (depending on S). Generally, as should be expected at a fixed grain size Y, the degree of the material heterogeneity for thermal neutrons (measured as $1/G$) increases faster when

the difference between the absorption cross-sections of the grains and matrix is larger and/or the volume content of grains (that is, their number) is higher.

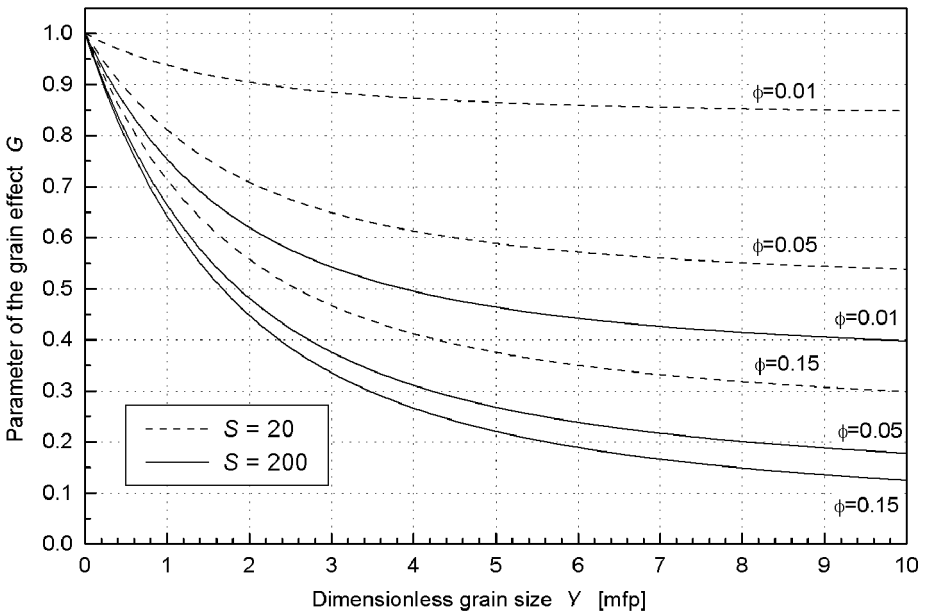

Fig. 2 a Parameter G of the grain effect as a function of the dimensionless size Y of the grain at fixed values of the ratios S and volume contents ϕ.

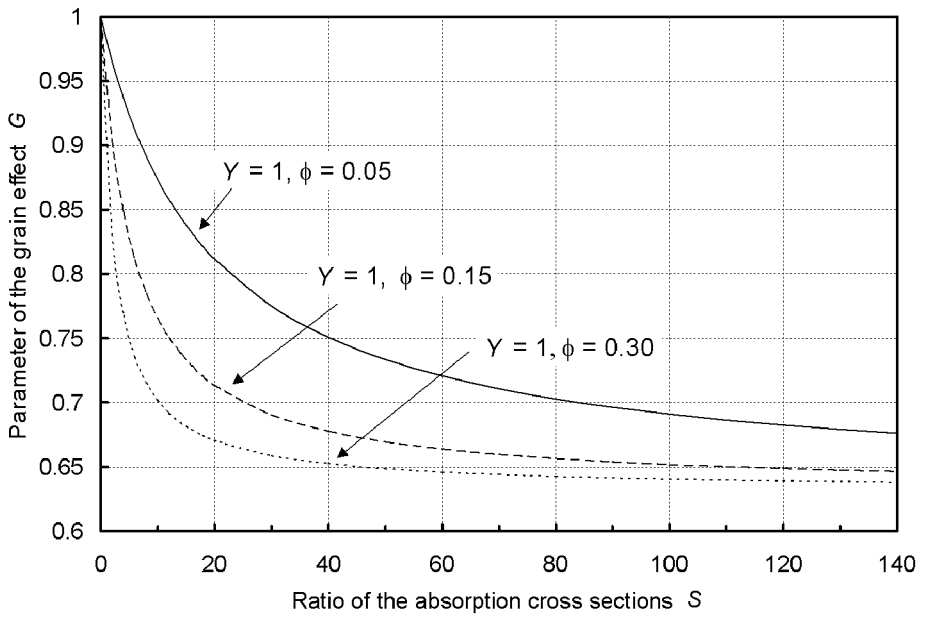

Fig. 2 b Parameter G of the grain effect as a function of the ratio S of the absorption cross-sections at a constant size Y of the grains and a fixed volume contents ϕ.

It is important to notice that for heterogeneous media, always $G < 1$, that is, the effective absorption cross-section is always lower than for a homogeneous material.

Until now, the theoretical analysis of the problem has been performed in the one-

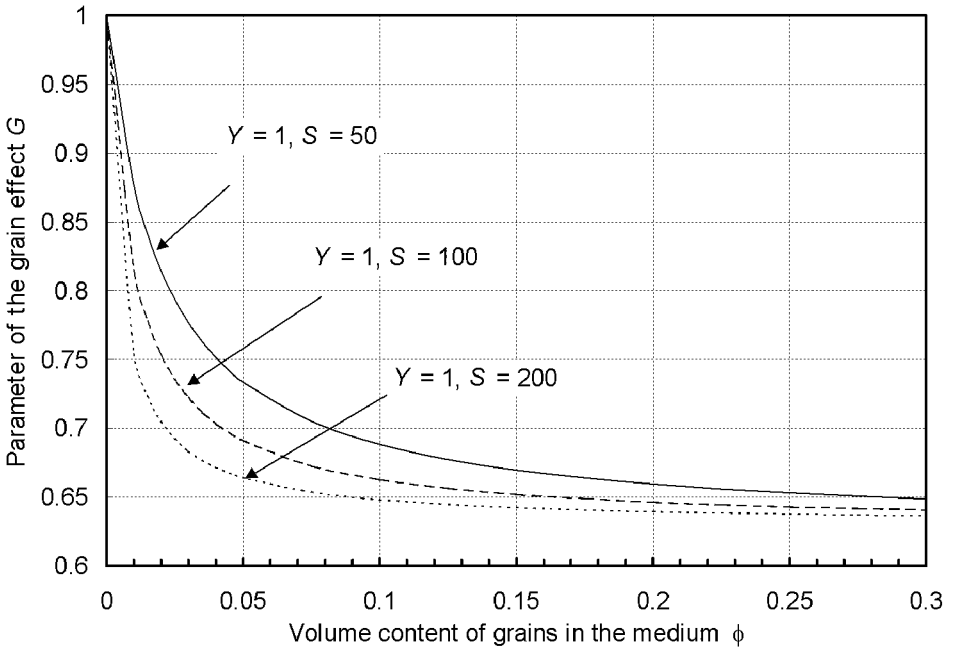

Fig. 2 c Parameter G of the grain effect as a function of the volume content ϕ of grains at a constant size Y of the grains and fixed ratios S.

speed approach to the thermal-neutron diffusion. However, thermal neutrons in real experimental conditions are characterised by an energy distribution and then average values are observed. For a comparison between the theoretical and experimental results, the energy-averaged neutron parameters must be used in the calculation. The grain parameter G is a function of three variables: $G = G(Y,\, S,\, \phi)$. Two of them, Y and S, depend on the neutron energy, because of the energy dependence of the cross-sections. The grain parameter, defined by the energy-averaged cross-sections, is

$$G_{av}(Y(E), S(E), \phi) = \frac{\langle \Sigma_a^{eff} \rangle}{\langle \Sigma_a^{hom} \rangle} \tag{17}$$

where E is the neutron energy and the bracket $\langle\ \rangle$ denotes the energy-averaged magnitude.

Let the energy distribution of the thermal-neutron flux in the investigated volume be approximated by the Maxwellian distribution:

$$M(E) = \frac{E}{E_T^2} e^{-E/E_T} \tag{18}$$

with $E_T = k_B T$, where k_B is the Boltzman constant and T is the absolute temperature. The distribution (18) is normalized to unity and the average thermal-neutron parameter, say $\langle P \rangle$, is defined as

$$\langle P \rangle \quad \equiv \quad \langle P(E) \rangle = \int_0^\infty P(E) M(E) dE \tag{19}$$

Thus, the energy-averaged, macroscopic absorption cross-sections of the mixtures are

$$\langle \Sigma_a^{hom} \rangle = (1-\phi)\langle \Sigma_{a_1}(E) \rangle + \phi \langle \Sigma_{a_2}(E) \rangle \tag{20}$$

In Case **A** we have:

$$\begin{aligned} \langle \Sigma_a^{eff} \rangle &= \langle (1-\phi)\Sigma_{a_1}(E) + \phi \tilde{\Sigma}_{a_2}(E) \rangle \\ &= (1-\phi)\langle \Sigma_{a_1}(E) \rangle + \phi \left\langle \frac{\Sigma_{a_2}(E)}{\overline{d}_2 \Sigma_{d_2}(E)} \left[1 - e^{-\overline{d}_2 \Sigma_{d_2}(E)} \right] \right\rangle \end{aligned} \tag{21}$$

In Case **B** the energy-averaged, effective absorption cross-section $\langle \Sigma_a^{eff} \rangle''$ is expressed by:

$$\begin{aligned} \langle \Sigma_a^{eff} \rangle'' &= \langle (1-\phi)\tilde{\Sigma}_{a_1}(E) + \phi \tilde{\Sigma}_{a_2}(E) \rangle \\ &= (1-\phi) \left\langle \frac{\Sigma_{a_1}(E)}{\overline{d}_1 \Sigma_{d_1}(E)} \left[1 - e^{-\overline{d}_1 \Sigma_{d_1}(E)} \right] \right\rangle + \phi \left\langle \frac{\Sigma_{a_2}(E)}{\overline{d}_2 \Sigma_{d_2}(E)} \left[1 - e^{-\overline{d}_2 \Sigma_{d_2}(E)} \right] \right\rangle \end{aligned} \tag{22}$$

and the grain parameter G''_{av} is

$$G''_{av} = \frac{\langle \Sigma_a^{eff} \rangle''}{\langle \Sigma_a^{hom} \rangle} \tag{23}$$

The experimental grain parameter is defined by

$$G^{exp} = \frac{\langle \Sigma_a^{exp} \rangle}{\langle \Sigma_a^{hom} \rangle} = \frac{\langle v\Sigma_a^{exp} \rangle}{\langle v\Sigma_a^{hom} \rangle} \tag{24}$$

where the energy-averaged thermal-neutron absorption rate $\langle v\Sigma_a \rangle$ is given by the relation

$$\langle v\Sigma_a \rangle = \int_0^\infty v\Sigma_a(E)M(E)dE = v_0\Sigma_a(v_0) \equiv v_0\Sigma_a \tag{25}$$

and $\langle \Sigma_a^{exp} \rangle$ or $\langle v\Sigma_a^{exp} \rangle$ is obtained from the experiment.

Further consideration will be limited to an analysis of the influence of the grain size on the absorption when the other parameters (S and ϕ) are fixed.

5 Laboratory measurement of the macroscopic absorption cross-section

Czubek's pulsed neutron method has been used to measure the absorption cross-section of the discussed heterogeneous materials. This method has been chosen because only one sample is needed to measure the thermal-neutron absorption cross-section Σ_a of the material. Notice that Σ_a is a parameter that characterizes an infinite medium, not a particular finite sample of a fixed size used in the measurement. Additionally, Czubek's method of the Σ_a measurement is independent of the scattering properties of the sample. The physical principles of the Σ_a measurement method, which uses a two-region geometry, have been recapitulated in [6]. The system consists of the investigated cylindrical sample of size $H_S = 2R_S$ surrounded by a cylindrical moderator ($H_M = 2R_M$) covered with a

cadmium shield, which assures vacuum boundary conditions for thermal neutrons. The geometry of the measurement is shown in Fig. 3. The sample-moderator system is irradiated by bursts of 14 MeV neutrons that are slowed down, and the time decay of the thermal-neutron flux $\varphi(t)$ is observed. Pulses from a ^{3}He detector are stored (during many consecutive cycles) in a multiscaler, and the decay constant λ of the fundamental exponential mode of the flux, $\varphi(t) \sim \exp(-\lambda t)$, is determined from the registered curve [7]. The experiment is repeated using different sizes H_M of the outer moderator. In this way the experimental dependence $\lambda = \lambda(x_M;\, R_S = const)$ is obtained, where $x_M = \frac{1}{R_M^2}$.

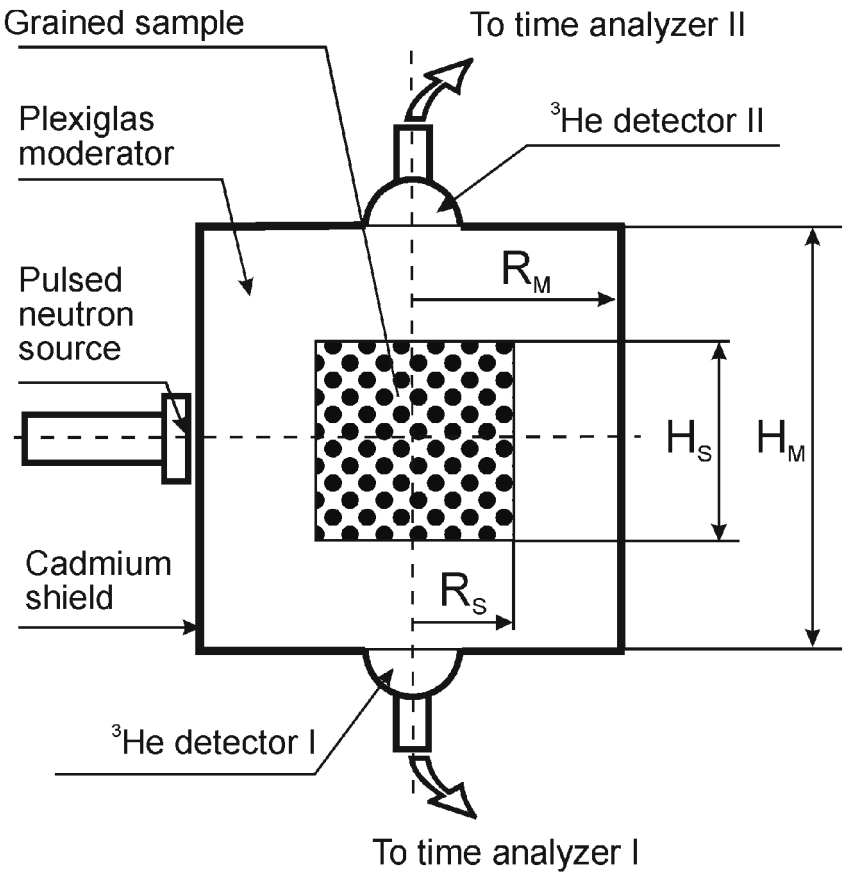

Fig. 3 The experimental set-up.

Another curve $\lambda^* = \lambda^*(x_M;\, R_S = const)$ is calculated based on the diffusion approximation for the thermal-neutron flux in the two-region cylindrical system [8], [9]. The curve $\lambda^*(x_M)$ is dependent on the size R_S of the inner sample and on the thermal-neutron parameters of the external moderator (that is, the absorption rate $\langle v\Sigma_{aM}\rangle$, the diffusion constant D_{0M}, and the diffusion cooling coefficient C_M) and, therefore, they have to be known with a high accuracy. The absorption rate $\langle v\Sigma_{aM}\rangle$ and the diffusion constant D_{0M} of Plexiglas, routinely used as the outer moderator in the measurements, are well established [10] and are quoted in [11]. Instead of the constant coefficient C_M used earlier, the correction function $C_M^*(\lambda^*)$ is now used. It results from the diffusion cooling of the thermal-neutron energy spectrum in the two-region system, in which the inner sample is a mixture of a hydrogenous and non-hydrogenous media [12]. The ordinate $\lambda_X = \langle v\Sigma_a^{exp}\rangle$

	Density [g cm^{-3}]	$\Sigma_a(v_0)$ [cm^{-1}]	$\frac{\Sigma_{a,Ag}(v_0)}{\Sigma_{a,Plexi}(v_0)}$
Silver, Ag	10.50	3.71053	195.8
Plexiglas, $(C_5H_8O_2)_n$	1.176	0.01895	195.8

Table 1 Physical characteristics of silver and Plexiglas.

of the intersection point of the curves $\lambda = \lambda(x_M)$ and $\lambda^* = \lambda^*(x_M)$ determines the absorption cross-section Σ_{aS} of the material of the inner sample:

$$\langle \Sigma_{aS} \rangle - \lambda_X \langle 1/v \rangle = 0, \tag{26}$$

where v is the neutron speed and the averages are over the thermal-neutron flux energy distribution. The standard deviation $\sigma(\lambda_X)$ of the intersection point λ_X is calculated using a computer simulation method [13].

6 Silver-in-Plexiglas models as heterogeneous samples

6.1 Design of the heterogeneous models

Well-defined models of heterogeneous materials have been constructed to perform a fully controlled experiment to investigate how the thermal-neutron absorption cross-section depends on the grain size of the material. The models fulfil the following assumptions:

(1) They consist of two materials: **I** and **II**.
(2) The difference between the absorption cross-sections of material **I** and **II** is significant; the highly absorbing centres (grains) of material **II** are embedded in a weakly absorbing material **I**.
(3) The grains **II** of regular shapes are regularly distributed in material **I**.
(4) The models differ from each other with respect to the grain size of material **II**, but its total mass contribution is kept constant.

Plexiglas has been used as the weakly absorbing material, and silver of a high purity has been chosen for making the highly absorbing grains. The physical characteristics of silver and Plexiglas are given in Table 1. Their macroscopic absorption cross-sections have been calculated at the most probable thermal-neutron velocity $v_0 = 2200$ m/s, based on the elemental compositions and on the microscopic absorption cross-sections given in nuclear data tables [14].

Three models of a regular cylindrical shape with $H_S = 2R_S = 9$ cm have been constructed. Each one consists of layers of two types: the pure Plexiglas layers are separated by layers with silver grains embedded in Plexiglas. The silver grains are regular cylinders of constant dimensions $H_{gr} = 2R_{gr}$, different in each model. Their total volume content in the samples is kept almost constant, about $\phi_{II} = 0.05$, corresponding to the mass contribution about $q_{II} = 0.32$. The characteristics of the three silver-in-Plexiglas models are given in Table 2.

Symbol of the Model	Size of the grain H_{gr} [mm]	Number of the grains in the Model	Mass contribution of silver q_{II}	Volume content of silver ϕ_{II}	Average chord of the grain $\overline{d}_2$ [cm]	Dimensionless size of the grain $\langle Y \rangle$
GR4	4	570	0.3199	0.0500	0.267	0.9563
GR6	6	168	0.3187	0.0498	0.400	1.4344
GR10	10	36	0.3169	0.0494	0.667	2.3906

Table 2 Characteristics of the silver-in-Plexiglas models.

In order to construct the sample of material with regularly distributed absorbing grains, the model has been considered as part of an infinite spatial grid, in which the grains represent the lattice points. A regular prism has been assumed as the grid. The small cylindrical grains are coaxial with the entire cylindrical model. The vertical and horizontal cross-sections of one of the models (with the biggest grains) are shown in Fig. 4. The geometric details of the other models can be found in [15]. The vertical distance between top and bottom of two neighbouring grains is approximately equal to the grain height H_{gr} . The first and the last (top and bottom) pure Plexiglas slices have the thickness about 1/2 of the grain height. The distribution of the grains in the horizontal cross-section has been selected from the square or hexagonal infinite grid. The slices containing grains can be rotated with respect to each other to observe a possible influence of the silver distribution on the effective absorption of the material.

6.2 Experimental results and discussion of a possible uncertainty

The size of the silver grains in the different silver-in-Plexiglas models varies, keeping always a constant volume content ϕ_{II} of silver. Thus, the models represent a heterogeneous material on which an effect of the varying grain size on the effective absorption can be measured and compared to the absorption of the homogeneous mixture.

The final experimental results $\langle \Sigma_a^{exp} \rangle$ for the three investigated heterogeneous media are reported in Table 3. These macroscopic absorption cross-sections $\langle \Sigma_a^{exp} \rangle$ can be compared with $\langle \Sigma_a^{hom} \rangle = 0.1805 cm^{-1}$ for the homogeneous mixture consisting of the same components, calculated at the silver content $\phi_{II} = 0.05$. The comparison clearly shows that the influence of the heterogeneity of the material on the effective, macroscopic absorption cross-section for thermal neutrons is significant, even in the case of the dense grid of the smallest silver grains, which is closest to a homogeneous material.

The absorption cross-section Σ_a is determined from the intersection point of the theoretical and experimental curves and, therefore, its accuracy $\sigma(\Sigma_a)$ within the theory of the measurement method depends on the accuracy both of the experimental points and of the neutron parameters used in the calculation. The accuracy $\sigma(\lambda_i)$ of the experimental points depends on the characteristics and possibilities of the experimental set-up and

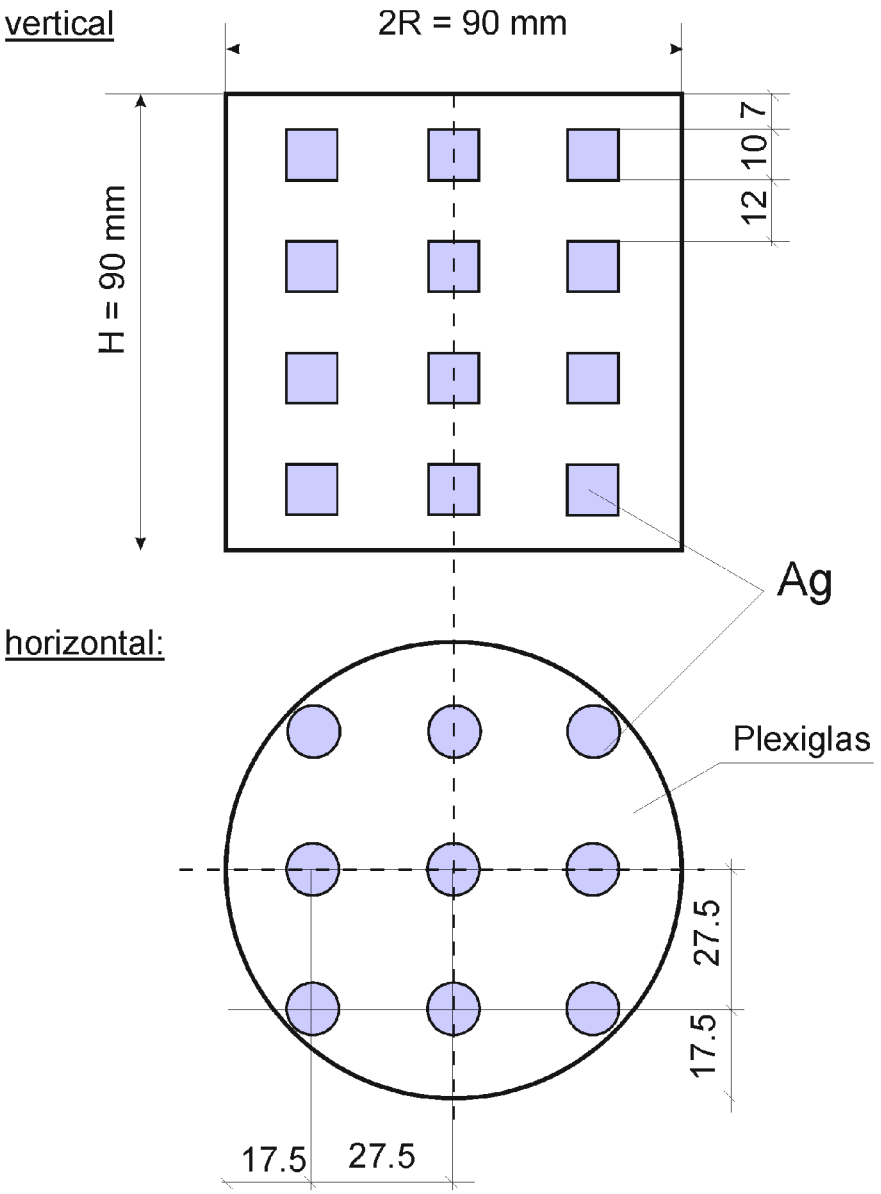

Fig. 4 Distribution of silver grains in Model GR10.

Model	$\langle v\Sigma_a^{exp}\rangle$ $\sigma(\langle v\Sigma_a^{exp}\rangle)$ $[s^{-1}]$	$\langle\Sigma_a^{exp}\rangle$ $\sigma(\langle\Sigma_a^{exp}\rangle)$ $[\mathrm{cm}^{-1}]$	$\frac{\sigma(\langle\Sigma_a^{exp}\rangle)}{\langle\Sigma_a^{exp}\rangle}$ [%]
GR4	26868 54	0.1083 0.0002	0.18
GR6	20743 78	0.0836 0.0003	0.36
GR10	14999 59	0.0605 0.0002	0.33

Table 3 Experimental results obtained for the silver-in-Plexiglas models.

on the precision of determination of the fundamental mode decay constant λ from the decay curve registered in the multiscaler. In the present experimental series, the determination of λ has been difficult. As λ describes the exponential decay, its value should be constant, independent of a shift t_0 of the analysed interval along the time axis, that is, $\lambda(t_0) = const$ (with a statistical accuracy). The heterogeneity of the sample leads to a stronger contamination with higher modes of the pulsed thermal-neutron flux, and makes more difficult the isolation of the fundamental mode. Therefore, the dependence $\lambda(t_0) = const$ has been always carefully tested in the interpretation of the experiments. Finally, the relative standard deviations $\sigma(\lambda_i)/\lambda_i$ have been no higher than 0.9 %.

Consider also an uncertainty in the size of the sample. Although the geometric dimensions H_S and R_S are known with a very high accuracy, how neutrons "see" this size can be a problem. Namely, the models contain the silver grain lattice in Plexiglas, which is also used as the outer moderator. In order to investigate this possible uncertainty, a new theoretical curve has been calculated, $\lambda^* = \lambda^*(x_M)$ at $2R_S$ increased by 0.2 cm. A new experimental result, $\langle\Sigma_a^{exp\text{-}n}\rangle$, has then been obtained for each model sample. (Notice that the change of the size $2R_s$ also changes the contributions ϕ_{II} and, in a consequence, the cross-sections $\langle\Sigma_a^{hom}\rangle$). The new experimental grain parameters, $G^{exp\text{-}n}$, have been obtained and the relative changes, $\varepsilon = (G^{exp\text{-}n} - G^{exp})/G^{exp}$, have been calculated. They appear negligible when compared with the statistical uncertainty $\sigma(\langle\Sigma_a\rangle)/\langle\Sigma_a\rangle$ of the measurements [15].

A separate problem is whether the model represents well a part of an infinite, regular lattice of grains. In order to test it we have made the following experiment for Model GR10, that is, for the sparsest lattice, where the influence of grains on the effective absorption cross-section is strongest. The sample has been enclosed only in a cadmium shield and the decay constant λ has been measured. Next, every other layer with the silver grains has been rotated 45 ° to introduce the intentional perturbation of the lattice (Fig. 5). The decay constant has been again measured. The results are following:
Regular lattice: $\lambda = 27\ 505\ \mathrm{s}^{-1}$, $\sigma(\lambda) = 68\ \mathrm{s}^{-1}$;
Perturbed lattice: $\lambda = 27\ 567\ \mathrm{s}^{-1}$, $\sigma(\lambda) = 85\ \mathrm{s}^{-1}$.

The measured decay constants are in full agreement within one standard deviation. This means that the perturbation of the lattice has not changed the thermal-neutron transport in the investigated volume. This suggests also that any possible error in the cut of the sample from the infinite lattice is not significant.

Finally, we can state that the factors considered above do not influence significantly the experimental results. The values listed in Table 3 can be treated as the measured, effective absorption cross-sections with errors on the level of two standard deviations.

6.3 Comparison of the theoretical and experimental results obtained for the silver-in-Plexiglas models

The theoretical approach presented in paragraphs 1 to 4 has been applied to an interpretation of the results of the experiments made on the three silver-in-Plexiglas models.

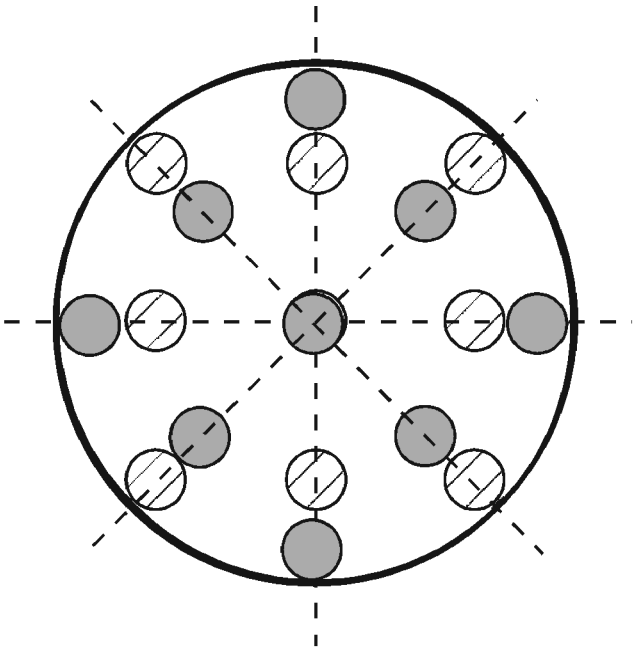

Fig. 5 Perturbed lattice of grains in Model GR10 (45^o rotated layers).

6.3.1 Case A: Grains in the matrix

The theoretical, effective, macroscopic absorption cross-sections $\langle\Sigma_a^{eff}\rangle$ of the three silver-in-Plexiglas models have been calculated from Eq. (21), and the absorption cross-section $\langle\Sigma_a^{hom}\rangle$ of the corresponding homogeneous material from Eq. (20). The energy dependence of the thermal-neutron, macroscopic absorption cross-sections of Plexiglas, $\Sigma_{a_1}(E)$, and of silver, $\Sigma_{a_2}(E)$, is described by a $1/v$ law. Therefore, these cross-sections are completely defined when given at only one energy (cf. Table 1). The diffusion cross-section Σ_{d2}, present in formula (21), contains the absorption and transport cross-sections of silver. The energy-dependent, scattering cross-section $\sigma_{s2}(E)$ of silver (given essentially by the free gas model formula) is, for thermal neutrons, very well approximated by a constant value equal to the free-atom scattering cross-section σ_{sf2}. Thus, the macroscopic scattering cross-section for silver is $\Sigma_{s2}(E) = \Sigma_{sf2} = 0.2978$ cm^{-1}. The scattering cosine $\mu_2(E)$ of silver is sufficiently accurately given by the approximate relation $\mu_2 = 2/(3A)$, where A is the relative-to-neutron atomic mass of silver (cf. [1]).

The calculated, energy-averaged, effective absorption cross-sections $\langle\Sigma_a^{eff}\rangle$ of the three models are listed in Table 4. The calculations have been performed for the silver volume content $\phi_{II} = 0.05$ at $E_T = 0.02526$ eV, corresponding to the experiment temperature $t = 20\,^\circ$C. The macroscopic absorption cross-section of the homogeneous mixture consisting of the same components with the same contributions has been quoted in paragraph 6.2.

Theoretical values of parameter G_{av} of the grain size effect have been calculated from Eq. (17). The experimental values G^{exp} of the parameter have been determined from the experimental data $\langle\Sigma_a\rangle^{exp}$ for the three silver-in-Plexiglas models from Eq. (24). The theoretical and experimental results are compared in Table 4. Plots of the grain effect

Model	$\langle\Sigma_a^{eff}\rangle$ [cm^{-1}]	G_{av}	G^{exp}	$\frac{G_{av}-G^{exp}}{G^{exp}}$ [%]
GR4	0.1164	0.6449	0.6000	7.48
GR6	0.0985	0.5457	0.4632	17.81
GR10	0.0754	0.4177	0.3352	24.61

Table 4 Comparison of the theoretical and experimental results obtained for the *silver-in-Plexiglas* models.

parameter calculated as a function of the grain size Y are shown in Fig. 6, where the three experimental values are also marked. The first curve, $G(Y)$, has been calculated from the one-speed approximation, Eq. (5) with (13) and (4), using the values of the cross-sections at the thermal-neutron energy E_T. The second curve, $G_{av}(Y)$, has been obtained from Eq. (17) with (21) and (20). The two functions present a difference between the theoretical results based on the one-speed treatment and on the approach in which all energy-dependent magnitudes are averaged over the thermal-neutron energy distribution. Although the curve $G_{av}(Y)$ is closer to the experimental points G^{exp} than the curve $G(Y)$, the prediction $G_{av}(Y)$ is still unsatisfactory for the experimental pointsG^{exp}. Two other curves in the plot are considered in the next paragraph.

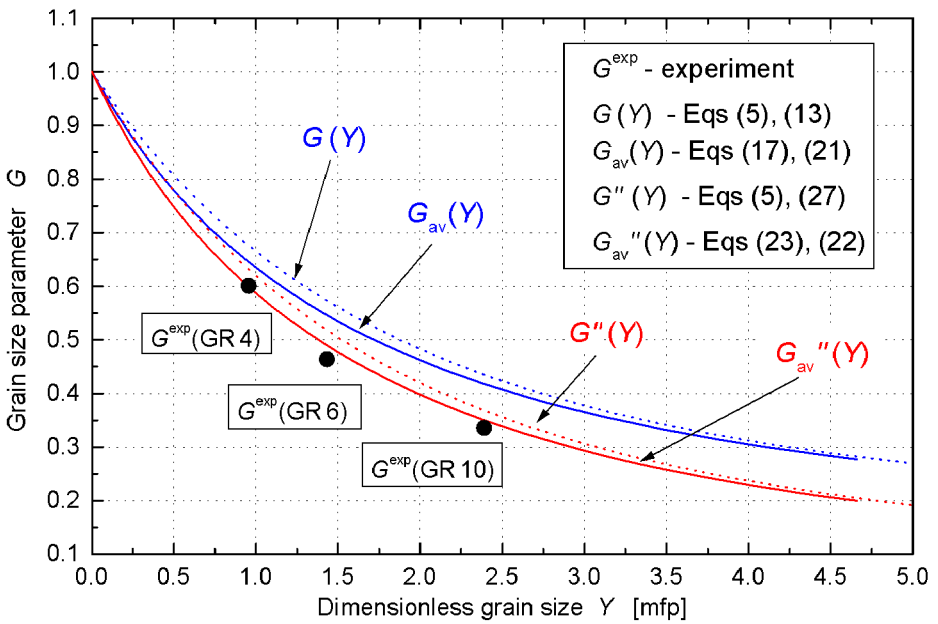

Fig. 6 Parameter of the grain size effect as a function $G(Y)$ of the grain size (at $S = 195.8$, $\phi = 0.05$) compared to the experimental results G^{exp} for three *silver-in-Plexiglas* models.

6.3.2 Case B: Two-grain medium

We consider Plexiglas as a medium built of grains, too. In this case, the volume treated as a Plexiglas grain is defined by the lattice points, without the space occupied in corners

by parts of the silver grains. The defined volume and its surface determine from Eq. (12) the average chord length $\overline{d}_1$ of the grain of the matrix (although such a treatment violates slightly the assumption of the convex curvature of the grain surface). Then the effective absorption cross-section $\tilde{\Sigma}_{a_1}$ of the weakly absorbing material is also calculated from Eq. (11). The effective cross-section of the material is expressed by:

$$\Sigma_a^{eff\prime\prime} = (1-\phi)\tilde{\Sigma}_{a_1} + \phi\tilde{\Sigma}_{a_2} \tag{27}$$

according to the definition in paragraph 2.

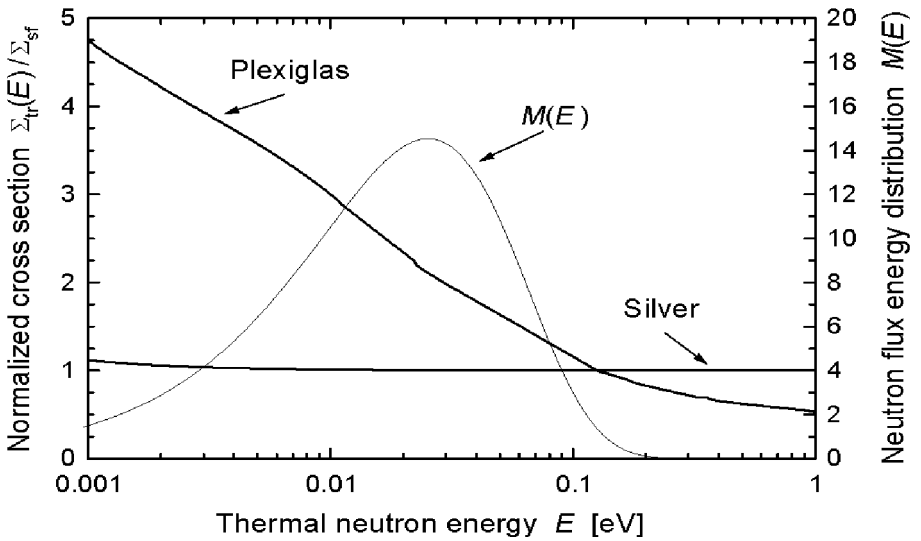

Fig. 7 Energy dependence of the thermal-neutron transport cross-section of Plexiglas and of silver, and the thermal-neutron flux energy distribution.

The energy-averaged, effective cross-section $\langle\Sigma_a^{eff}(E)\rangle''$ can be calculated when the dependence $\tilde{\Sigma}_{a_1}(E)$ is known. It contains not only the absorption cross-section $\Sigma_{a_1}(E)$ but also the energy-dependent transport cross-section $\Sigma_{tr1}(E)$ of Plexiglas [cf. Eqs. (11), (9) and (8)]. As in any hydrogenous material, the scattering cross-section and the average cosine of the scattering angle are strongly dependent on the thermal-neutron energy. The functions $\Sigma_{s1}(E)$ and $\mu_1(E)$ have been obtained in the same way as in [16], following Granada's model of the slow-neutron scattering kernel [17], [18], [19]. The dependence $\Sigma_{tr1}(E)$ is shown in Fig. 7, together with the thermal neutron distribution $M(E)$. Additionally the silver cross-section $\Sigma_{tr2}(E)$ is also plotted.

Theoretical values of the parameter of the grain size effect G''_{av}, resulting from the present approach to the considered three silver-in-Plexiglas models, are specified in Table 5.

According to assumption (27), a new set of curves has been obtained, $G''(Y)$ and $G''_{av}(Y)$, corresponding to the one-velocity treatment [Eq. (5) with (27)] and to the energy averaging [Eq. (23) with (22)], respectively. They are plotted in Fig. 6 as the two lowest lines. In order to plot these new functions versus Y, the lengths $\overline{d}_1$ have been expressed using the average chord lengths $\overline{d}_2$ of the corresponding silver grains, $\overline{d}_1 = k_m\overline{d}_2$, where

Model	$\langle\Sigma_a^{eff}\rangle''$ [cm^{-1}]	G''_{av}	$\frac{G''_{av}}{G_{av}}$	$\frac{G''_{av}-G^{exp}}{G^{exp}}$ [%]
GR4	0.1080	0.5983	0.9277	- 0.28
GR6	0.0873	0.4837	0.8864	4.43
GR10	0.0634	0.3512	0.8408	4.77

Table 5 Comparison of the results of the two-grain theory with the experimental data.

k_m is a constant dependent on the sample, that is, on the particular spatial distribution of grains. The new approach, especially $G''_{av}(Y)$, gives much better agreement with the experimental results G^{exp}.

7 Rock–fluid samples

When rock materials are investigated, the sample usually contains grains which create heterogeneity. The experiments on the artificial rock material (silicon, Si) and on the natural rock material (diabase) have been performed to examine the influence of the granulation on the Σ_a measurement. The samples have been prepared as mixtures of grained materials with aqueous solutions of boric acid, H_3BO_3.

The thermal-neutron absorption rates $\langle v\Sigma_a^{exp}\rangle$ of the complex samples have been measured with Czubek's method, as outlined in paragraph 5. The absorption rate of the homogeneous mixture $\langle v\Sigma_a^{hom}\rangle$ has been obtained from Eq. (26) and Σ_a^{hom} has been calculated from the following formula:

$$\begin{aligned}\Sigma_a^{hom} &= \rho\Big[q_{rock}\Sigma^M_{rock} + (1-q_{rock})\Sigma^M_{fluid}\Big] \\ &= \rho\Big\{q_{rock}\Sigma^M_{rock} + (1-q_{rock})\Big[(1-k)\Sigma^M_{H_2O} + k\Sigma^M_{H_3BO_3}\Big]\Big\}\end{aligned} \tag{28}$$

which results from Eq.(1), and where ρ is the mass density of the complex sample, q_{rock} is the mass fraction of the rock in the complex *rock-fluid* sample, k is the mass fraction of H_3BO_3 in the fluid, and $\Sigma_x^M = \Sigma_a/\rho$ is the relevant, mass absorption cross-section calculated on the basis of the elemental composition and the microscopic absorption cross-sections ([14], except for boron). The absorption cross-section of the boric acid H_3BO_3 was measured [20] in our Lab to avoid an uncertainty introduced by the fluctuating isotopic ratio of natural boron. Finally, the experimental grain parameter G^{exp} has been obtained from Eq. (24).

The theoretical grain parameter G_{av} has been calculated from Eq. (17), assuming Case **A** (Eq. 21), that is, that the grains of the rock (a weak absorber) are embedded in the matrix (a strong absorber).

7.1 Silicon as the artificial rock material of grains

An artificial rock material allows us

(1) to create more realistic experimental conditions, that is, a sample that contains grains of a fluctuating size, spread irregularly (not preserving a regular lattice, as in the model samples), and

(2) to keep exactly known thermal-neutron parameters of the contributing materials.

High purity silicon (0.9999 Si) has been used. Its thermal-neutron mass macroscopic cross-sections are:
Absorption: $\Sigma_a^M(v_0) = 0.00367 \pm 0.00006$ cm^{2}g^{-1}.
Scattering: $\Sigma_s^M(v_0) = 0.04382 \pm 0.00004$ cm^{2}g^{-1}
([21], [14]). The complex samples have been made of two different grain sizes embedded in various H_3BO_3 solutions. The specification of the samples is given in Table 6.

An example of the theoretical dependence of the grain parameter G_{av} for the investigated samples is shown in Fig. 8 (the upper line). The parameter is plotted as a function of the grain diameter, $2R_{gr}$, with the other variables fixed according to the experimental conditions. The theoretical grain parameter is, in practice, equal to unity in the considered interval of the grain size. The exact values for the samples are given in Table 6. For sample Si-07, only the results obtained for the lowest and highest concentrations of the H_3BO_3 solutions used are shown. In the calculation, the grain sizes $\overline{d}$ have been defined by the average chords relevant to the mean diameters of the grains used, that is, 0.6 mm and 1.7 mm for the grains of (0.5 to 0.7) and of (1.4 to 2.0) mm of sieve mesh, respectively.

Sample Code	Silicon grain size d [mm of sieve mesh]	Nominal concentration of boric acid k [wt. %]	Volume contribution of silicon ϕ	$\frac{1}{S} = \frac{\Sigma_{a_1}}{\Sigma_{a_2}}$	$\langle\Sigma_a^{hom}\rangle$ Eq. (20) [cm^{-1}]	G_{av} Eq.(17)
Si-07c	0.5 ÷ 0.7	1.2	0.497	12.89	0.0529	0.9998
Si-07d	0.5 ÷ 0.7	3.5	0.493	32.86	0.1298	0.9999
Si-2	1.4 ÷ 2.0	1.2	0.474	12.89	0.0549	0.9996
Si-2a	1.4 ÷ 2.0	2.0	0.479	19.81	0.0817	0.9997
	Density of silicon $\rho_{Si} = 2.3280 \pm 0.0002$ g cm^{-3}					

Table 6 Specification of the complex samples (mixtures of silicon grains with the H_3BO_3 solutions) and the theoretical grain parameter.

The thermal-neutron absorption rates $\langle v\Sigma_a\rangle^{exp}$ of the complex samples have been measured. The absorption rate of the homogeneous mixture $\langle v\Sigma_a\rangle^{hom}$ and the experimental parameter G^{exp} has been obtained. The experimental absorption cross-sections of pure silicon, $\Sigma^{exp}(v_0)$, has been evaluated from the usual procedure in Czubek's method. The ratio of the obtained experimental value to the cross-section of silicon, $\Sigma^{exp}(v_0)/\Sigma_{Si}(v_0)$,

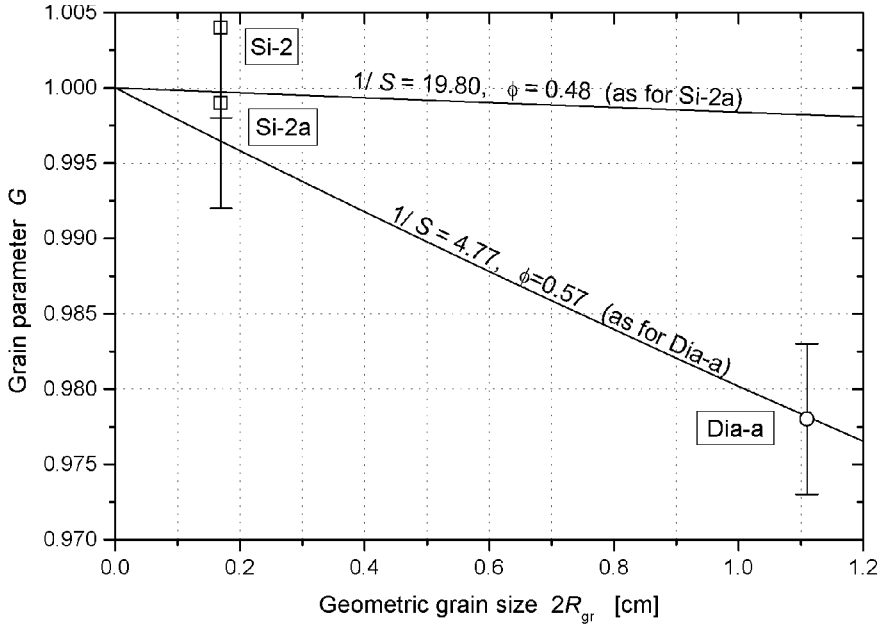

Fig. 8 Theoretical grain parameter G_{av} as a function of the geometric grain size and example of the experimental results G^{exp} (with the one standard deviation marked) for the silicon and diabase complex samples.

has been obtained. Details of the experiments and calculation procedures can be found in [12]. The results are collected in Table 7. No effect of heterogeneity is observed for the complex samples tested, with the silicon grains of about 0.6 and 1.7 mm, the silicon contribution $\phi \approx 0.5$, and the absorption cross-section ratios 1/S ≈ 13 and 1/S ≈ 20. Both the grain parameter G^{exp} for the complex sample and the ratio $\Sigma^{exp}(v_0)/\Sigma_{Si}(v_0)$ for the material of interest are equal to unity within the one standard deviation, which means that the experiment has confirmed the theoretical predictions on the homogeneity of the prepared complex media.

7.2 Diabase as the natural grained rock material

Diabase samples used in the present neutron measurements were taken from the compact deposit exploited by "Niedźwiedzia Góra" Quarry (Quarries of Natural Resources, Krzeszowice near Kraków, Poland). The absorption cross-section $\Sigma_a = \Sigma_R$ of diabase (as for infinite, homogeneous medium) was measured in our Lab, using Czubek's method, in an independent experiment [22], [23] on the fine samples. The scattering cross-section Σ_s has been calculated [21], [14] according to a typical elemental composition of diabase [24]. The following mass cross-sections have been obtained:
Absorption: $\Sigma_a^M(v_0) = 0.00890 \pm 0.00015$ cm^{2}g^{-1}
Scattering: $\Sigma_s^M(v_0) = 0.09428 \pm 0.00011$ cm^{2}g^{-1}.

The same material of granulation between 6.3 and 12.8 mm of sieve mesh has been used to calculate and measure the grain effect. The complex samples of the diabase grains and aqueous solutions of boric acid H_3BO_3 were prepared. The list of the complex

Sample Code	Complex sample (Si + absorber)			Silicon		
	$\langle v\Sigma_a\rangle^{hom}$	$\langle v\Sigma_a\rangle^{exp}$	G^{exp}	$\Sigma^{Mexp}(v_0)$	$\Sigma^{exp}(v_0)$	$\frac{\Sigma^{exp}(v_0)}{\Sigma_{Si}(v_0)}$
	$\sigma(\langle v\Sigma_a\rangle^{hom})$	$\sigma(\langle v\Sigma_a\rangle^{exp})$	$\sigma(\mathrm{G}^{exp})$	$\sigma(\Sigma^{Mexp})$	$\sigma(\Sigma^{exp})$	$\sigma(\Sigma^{exp}/\Sigma_{Si})$
	[s^{-1}]	[s^{-1}]		[cm^2g^{-1}]	[cm^{-1}]	
Si-07c	13 115	13 050	0.995	0.00340	0.00791	0.99
	51	62	0.006	0.00031	0.00072	0.09
Si-07d	32 185	32 222	1.001	0.00374	0.00870	1.02
	143	178	0.007	0.00090	0.00210	0.25
Si-2	13 621	13 678	1.004	0.00389	0.00906	1.06
	53	69	0.006	0.00034	0.00080	0.10
Si-2a	20 273	20 250	0.999	0.00355	0.00827	0.97
	85	107	0.007	0.00055	0.00127	0.15

Table 7 Comparison of the experimental results for silicon complex samples with the data for the homogeneous media.

Sample Code	Nominal concentration of boric acid solution	Volume contribution of the rock ϕ	$\frac{1}{S}=\frac{\Sigma_{a_1}}{\Sigma_{a_2}}$	$\langle\Sigma_a^{hom}\rangle$ Eq.(20)	G_{av} Eq.(17)
Dia-a	1.3	0.572	4.8	0.0570	0.978
Dia-b	2.0	0.559	6.9	0.0783	0.985
Dia-c	2.5	0.557	8.4	0.0932	0.988
	Density of diabase $\rho_R = 2.7680 \pm 0.0002$ g cm^{-3}				

Table 8 Specifications of the complex samples: mixtures of diabase grains (6.3 ÷ 12.8 mm of sieve mesh) with the H_3BO_3 solutions, and the theoretical grain parameter.

samples and the theoretically calculated grain parameters G_{av} are given in Table 8. The mean size of the diabase grain in each sample has been estimated as the diameter $2R_{gr}$ of an equivalent sphere, based on the number and total mass of the grains contained. An example of the theoretical grain parameter as a function of the grain size is plotted in Fig. 8 (the lower line). The contributions of the components and the ratio of the absorption cross-sections have been assumed as for the real sample, Dia-a.

The measurements of the effective absorption cross-sections of the complex samples and the evaluation of the experimental cross-section for diabase have been performed in the same way as described in the previous paragraph for the silicon samples. The results are collected in Table 9. The theoretical and experimental grain parameters fluctuate about 0.98. The small discrepancies between them can result from the necessary approximation of the grain size in the theoretical calculation. The heterogeneity effect, although weak, is clearly seen in a comparison with the results for the samples of fine silicon (cf. Fig. 8). The experimental cross-section of diabase itself, obtained from

Sample Code	Complex sample (Diabase + absorber) $\langle v\Sigma_a\rangle^{hom}$ $\sigma(\langle v\Sigma_a\rangle^{hom})$ [s^{-1}]	$\langle v\Sigma_a\rangle^{exp}$ $\sigma(\langle v\Sigma_a\rangle^{exp})$ [s^{-1}]	G^{exp} $\sigma(G^{exp})$	Diabase $\Sigma^{Mexp}(v_0)$ $\sigma(\Sigma^{Mexp})$ [cm^2g^{-1}]	$\Sigma^{exp}(v_0)$ $\sigma(\Sigma^{exp})$ [cm^{-1}]	$\frac{\Sigma^{exp}(v_0)}{\Sigma_R(v_0)}$ $\sigma(\Sigma^{exp}/\Sigma_{Si})$
Dia-a	14 192	13 881	0.978	0.00801	0.02217	0.90
	69	35	0.005	0.00016	0.00044	0.02
Dia-b	19 470	18 989	0.975	0.00749	0.02073	0.84
	87	101	0.007	0.00036	0.00100	0.04
Dia-c	23 141	22 566	0.975	0.00721	0.01996	0.81
	102	118	0.007	0.00044	0.00122	0.05

Table 9 Comparison of the experimental results for diabase complex samples with the data for the homogeneous media.

the standard interpretation of the measurement (assuming a homogeneous medium) is, however, underestimated even up to 20 %. The value of the underestimation depends on the ratio of the absorption cross-sections of the components in the complex samples. The higher is the ratio $1/S$, the lower is the interpreted cross-section Σ^{exp} of diabase, which is seen from the data in Tables 8 and 9. This behaviour is in agreement with the predictions of the theoretical model.

8 Conclusions

The theoretical approach to the thermal-neutron effective absorption in the type of heterogeneous medium considered here has been verified experimentally on dedicated model samples and on natural rock samples. The heterogeneity effect depends on few parameters: on the ratio S of the absorption cross sections of the components, on their scattering properties, on the grain size, and on the mass (or volume) contributions of the components.

A comparison of the influence of the grain size on the absorption in different samples can be done if the size is not expressed geometrically but using the neutron diffusion units. The thermal-neutron diffusion mean free path l_d in a given material is defined by the macroscopic diffusion cross section, $l_d = 1/\Sigma_d$. The grain size Y is referred to the geometrical dimension (the average chord length $\overline{d}$) and to the neutron mean free path, as shown in Eq.(16). The grain sizes Y in the particular samples are listed in Table 10.

For the *silver-in-Plexiglas* samples, the geometrical relations are precisely defined and it is possible to define accurately the grain size of the matrix material. The grain sizes Y for the two components are comparable and, as found earlier (paragraph 6.3.2), the medium in this case should be considered rather as the two-grain system.

For the *rock–fluid* samples, only the mean geometrical grain size is known, the spaces between the grains (filled with the matrix material) are highly irregular, and the size of

Sample	GR10	GR6	GR4	Si-07	Si-2	Dia
$\langle Y \rangle_{grain}$	2.39	1.43	0.96	~ 0.004	~ 0.012	~ 0.2
$\langle Y \rangle_{matrix}$	3.96	3.04	1.49	~ 0.12	~ 0.34	~ 2.0
$\frac{\langle Y \rangle_{matrix}}{\langle Y \rangle_{grain}}$	1.7	2.1	1.6	~ 30	~ 30	~ 10
Adequate theoretical model	Two-grain system			Homogeneous medium		Grains in the matrix

Table 10 Ratio of the dimensionless grain sizes $\langle Y \rangle$ in the particular samples.

the matrix grain is only estimated. In the case of the silicon samples, the ratio of the Y_1 and Y_2 sizes indicates that the system should be considered as the Si grains in the fluid matrix. Additionally, the geometrical sizes of grains are very small in comparison to the corresponding neutron mean free paths. Both the theoretical grain-in-the-matrix model and the experiment confirm in this case that the samples are homogeneous from the point of view of the neutron diffusion. The diabase grains are much greater, but their Y size is still one order lower than the estimated matrix grain size. Therefore, the grain-in-the-matrix mode is still applicable. The theoretical calculation and the experiment show a very weak grain effect G due to a low ratio of Σ_a of highly and weakly absorbing components, two orders lower than in the case of the *silver-in-Plexiglas* models (cf. Tables 8 and 1).

The general behaviour is as follows: the thermal-neutron absorption cross-section of any heterogeneous medium is always lower than a homogeneous one consisting of the same components. This effect can be a source of an **underestimation** of the absorption cross-section of the rock material when coarse-grain samples are used in laboratory measurements, as it has been proved in the paper. The opposite effect, an **overestimation** of the calculated absorption cross-section of a geological formation can happen if this medium is treated as homogenous material, while in fact it contains concretions of strongly differing absorption. Similarly, for such formation, an overestimated value can also be obtained experimentally from a measurement on its sample which is perfectly homogenised.

Acknowledgments

We wish to thank Prof. Nils G. Sjöstrand from Dept. of Reactor Physics at the Chalmers University of Technology (Göteborg, Sweden) for stimulating discussions on the problem.

We thank our colleagues, M.Sc. J. Dabrowska, Eng. A. Kurowski, Eng. J. Burda, and Mr. W. Janik, for their participation in the measurements.

The work was partly sponsored by the State Committee for Scientific Research of Poland (Project No. 9 T12B 027 16).

References

[1] K.H. Beckurts, K. Wirtz: *Neutron Physics*, Springer, Berlin, 1964.

[2] J.A. Czubek, Drozdowicz, B. Gabańska, A. Igielski, E. Krynicka-Drozdowicz, U. Woźnicka: "Advances in absolute determination of the rock matrix absorption cross section for thermal neutrons", *Nucl. Geophys.*, Vol. 5, (1991), pp. 101–107.

[3] K.M. Case, F. Hoffmann, G. Placzek: *Introduction to the Theory of Neutron Diffusion. Vol. I.*, Los Alamos Scientific Laboratory, 1953.

[4] J. Molina, M.C. Lopes: "The effect of scattering on thermal neutron self-shielding factors of infinite cylindrical probes", *Kerntechnik*, Vol. 51, (1987), pp. 194–196.

[5] J. Molina, M.C. Lopes: "A new approach to the neutron self-shielding factor with multiple scattering", *Kerntechnik*, Vol. 52, (1988), pp. 197–199.

[6] J.A. Czubek, K. Drozdowicz, B. Gabańska, A. Igielski, E. Krynicka, U. Woźnicka: "Thermal neutron macroscopic absorption cross section measurement applied for geophysics", *Progress in Nucl. Energy*, Vol. 30, (1996), pp. 295–303.

[7] K. Drozdowicz, B. Gabańska, E. Krynicka: "Fitting the decaying experimental curve by a sum of exponentials", In: *Rept. INP No. 1635/AP*, Institute of Nuclear Physics, Kraków, 1993.

[8] U. Woźnicka: "Solution of the thermal neutron diffusion equation for a two-region system by perturbation calculation", *J.Phys. D: Appl. Phys.*, Vol. 14, (1981), pp. 1167–1182.

[9] K. Drozdowicz, U. Woźnicka: "Energy corrections in pulsed neutron measurements for cylindrical geometry", *J.Phys. D: Appl. Phys*, Vol. 16, (1983), pp. 245–254.

[10] K. Drozdowicz, U. Woźnicka: "High-precision thermal neutron diffusion parameters for Plexiglas", *J.Phys. D: Appl. Phys.*, Vol. 20, (1987), pp. 985–993.

[11] E. Krynicka, K. Drozdowicz, B. Gabańska, W. Janik, J. Dabrowska: "Measurements of the thermal neutron absorption Σ_a of model systems (reference KCl solutions) in two-region geometry", In: *Rept. INP No. 1857/PN*, Institute of Nuclear Physics, Kraków, 2000, http://www.ifj.edu.pl/reports/2000.html.

[12] K. Drozdowicz, E. Krynicka, U. Woźnicka, A. Igielski, A. Kurowski: "The thermal neutron absorption of mixtures of hydrogenous and non-hydrogenous substances measured in two-region geometry", *Rept. INP No. 1891/PN*, Institute of Nuclear Physics, Kraków, 2001, http://www.ifj.edu.pl/reports/bib2001.html.

[13] Krynicka-E. Drozdowicz: "Standard deviation of the intersection point for two statistically uncertain curve", *Rept. INP No.1212/PM*, Institute of Nuclear Physics, Kraków, 1983.

[14] S.F. Mughabghab, M. Divadeenam, N.E. Holden: "Neutron Cross Sections", *Neutron Resonance Parameters and Thermal Cross Sections. Vol. 1. Part A.*, Academic Press, New York, 1981.

[15] K. Drozdowicz, B. Gabańska, A. Igielski, E. Krynicka, U. Woźnicka: "A pulsed measurement of the effective thermal neutron absorption cross-section of a heterogeneous medium", *Ann. Nucl. Energy*, Vol. 28, (2001), pp. 519–530.

[16] K. Drozdowicz: "The diffusion cooling coefficient for thermal neutrons in Plexiglas", *J. Phys. D: Appl. Phys.*, Vol. 31, (1998), pp. 1800–1807.

[17] J.R. Granada: "Slow-neutron scattering by molecular gases: A synthetic scattering function", *Phys. Rev.*, Vol. B 31, (1985), pp. 4167–4177.

[18] J.R. Granada, V.H. Gillette: "A review of a synthetic scattering function approach to the thermal and cold neutron scattering kernels of moderator materials", *J. Neutr. Research*, Vol. 7, (1999), pp. 75–85.

[19] K. Drozdowicz: "Thermal neutron diffusion parameters dependent on the flux energy distribution in finite hydrogenous media", *Rept. INP No. 1838/PN*, Institute of Nuclear Physics, Kraków, 1999.

[20] E. Krynicka, B. Gabańska, U. Woźnicka, M. Kosik-Abramczyk: "Measurements of the thermal neutron absorption Σ_a of boron of unknown isotopic ratio", *Rept. INP No. 1860/PN*, Institute of Nuclear Physics, Kraków, 2000, http://www.ifj.edu.pl/reports/bib2000.html.

[21] K. Drozdowicz, E. Krynicka: "Thermal neutron diffusion parameters in homogeneous mixtures", *Rept. INP No. 1694/PN*, Institute of Nuclear Physics, Kraków, 1995.

[22] U. Woźnicka, E. Krynicka, K. Drozdowicz, M. Kosik, W. Janik: "Influence of granulation of the diabase sample on the thermal neutron Σ_a measurement", *Rept. INP No. 1893/PN*, Institute of Nuclear Physics, Kraków, 2001, http://www.ifj.edu.pl/reports/2001.html.

[23] B. Gabańska, E. Krynicka, U. Woźnicka: "Effect of a crushing degree of the rock sample on the thermal neutron absorption cross section measurement", *Nafta-Gaz*, Vol. 5, (2002), pp. 231–239.

[24] A. Polański, K. Smulikowski: *Geochemia*, Wyd. Geologiczne, Warszawa, 1969, pp. 60.